Alkane Solvent-Derived Acylation Reaction Driven by Electric Fields

Xiye Wang[1‡], Boyuan Zhang[2‡], Brandon Fowler[1], Latha Venkataraman[1,2*], and Tomislav Rovis[1*]

[1] Department of Chemistry, Columbia University, New York, NY, USA. [2] Department of Applied Physics and Applied Mathematics, Columbia University, New York, NY, USA.

KEYWORDS. Electric Field Catalysis, Autoxidation, Green Chemistry, Single-Molecule Conductance.

ABSTRACT: Electric field acceleration of alkyl hydroperoxide activation to acylate amines in the scanning tunneling microscopy-break junction (STM-BJ) is reported. Alkyl hydroperoxide mixtures, generated from hydrocarbon autoxidation in air, were found to be competent reagents for the functionalization of gold surfaces. Intermolecular coupling on the surface in the presence of amines was observed, yielding normal alkyl amides. This novel mode of alkyl hydroperoxide activation to generate acylium equivalents was found to be responsive to the magnitude of the bias in the break junction, indicating an electric field influence on this novel reactivity.

Electric fields influence reaction profiles by stabilization of charge-separated transition states. This hypothesis has long been supported by computational studies in enzymatic catalysis, where the high efficiencies of enzymes can only be fully accounted for when electric field stabilization of the reaction transition state is considered.[1,2] Although mostly investigated computationally,[3,4] a body of experimental validations of this electric field effect has recently emerged in enzymatic catalysis,[5,6] scanning tunneling microscope (STM), electrical devices,[7] and organic reactions.[8] These examples highlight the potential for harnessing oriented electric fields as a new paradigm in biasing reaction rate,[9] chemoselectivity,[10] and stereoselectivity.[11] However, synthetically viable control and manipulation of the field remain rare and challenging.

Several recent examples demonstrate that an external electric field (EEF) in an STM-BJ catalyzes chemical reactions (Scheme 1). Darwish, Ciampi, Diez-Perez, and Coote *et al.* showed that an oriented EEF applied between an STM gold tip and a gold substrate can enhance the rate of a Diels-Alder reaction.[12] One of us reported the first bulk solution isomerization catalyzed by an electric field, using the STM-break junction (STM-BJ) technique to influence the isomerization of a *cis*-[3]cumulene to a *trans*-[3]cumulene.[13] The increased isomerization rate and perturbation of product equilibrium by the EEF demonstrate that the electric field can affect both reaction kinetics and thermodynamics.

Herein we report the unusual reactivity behavior of *N,N′* -dimethylethylenediamine (DMEDA) under EEF in the STM-BJ, where mono-acylation resulting in amide products bearing normal alkyl chains of various lengths is detected in tetradecane (Figure 1a). In order to monitor the reaction *in situ*, measurements of conductance of the reactants and products in bulk solution were recorded. The conductance was measured via the STM-BJ technique at room temperature. A gold tip was driven in and out of contact with a gold substrate using tetradecane (TD) as the solvent. The electric field was applied between a gold STM tip and a gold substrate, while the strength of the field was modulated by the bias applied.

Logarithmically binned one-dimensional (1D) conductance histograms compiled from thousands of measured traces in TD at a modest bias of 100 mV for DMEDA showed one conductance peak at 1.1×10^{-3} G_0 at the beginning of the measurement; a second peak was observed growing over this

Scheme 1. Chemical reactions catalyzed by EEF

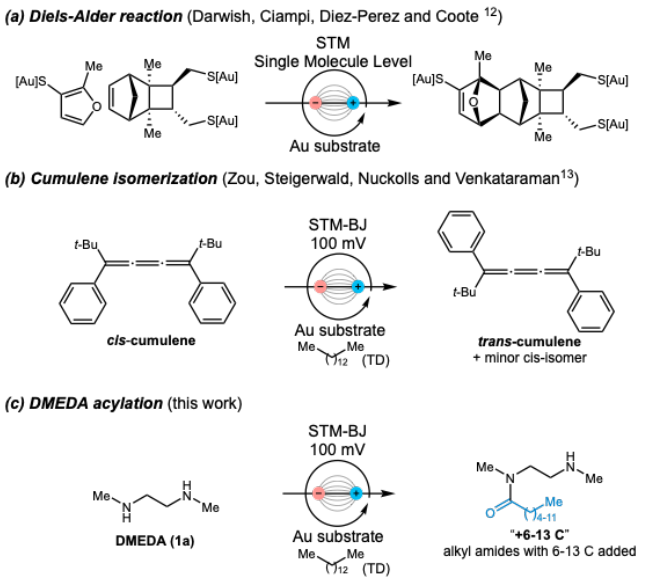

timeframe at a conductance of 0.9×10^{-4} G_0 (Figure 1b and SI Figure 2-2). The corresponding two-dimensional (2D) conductance-displacement histograms are shown in SI Figure 2-1. We attribute the higher conductance peak with shorter plateau to the reactant DMEDA and the lower conductance peak with longer plateau to the major products of the *in situ* reaction. Subsequent analysis of the reaction mixture by LC-MS[E] identified the major products in the reaction as a series of monoacylated DMEDA derivatives bearing alkyl chains of different lengths (Figure 1c, SI Figure 2-9 to 2-22). The reactivity on the gold substrate alone, albeit lower than with an applied field in the STM-BJ (*vide infra*), was amenable to scale-up using a larger gold-coated substrate. A sufficient quantity of the products was generated in this fashion; separation and isolation of the reaction mixture ultimately led to the product structural assignment as mono *n*-alkyl amides of DMEDA (SI Figure 2-3 to 2-7). Independently synthesized authentic product standards were found to be a match for the product, as their LC retention times were in agreement with products in the STM reaction (SI Figure 2-23). Conductance measurements of *ex-situ*

synthesized product in the STM-BJ accurately matched the shape and intensity measured for the low conductance peak formed over time in the DMEDA solution. Similarly, the 2D conductance histograms measured for product standards also matched the reaction 2D histogram (SI Figure 2-1).

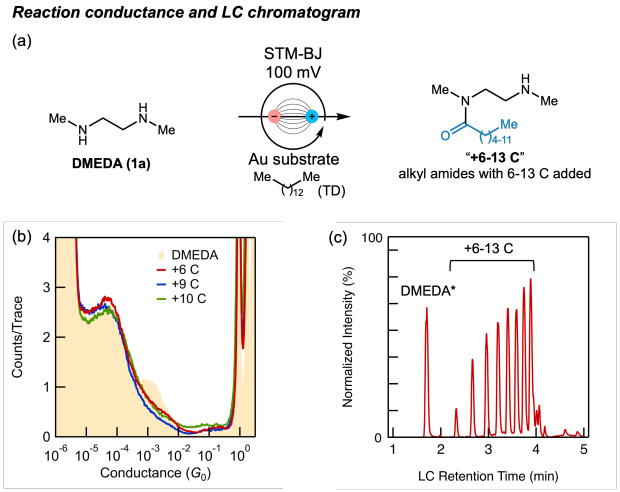

Figure 1. **Reaction conductance and LC chromatogram.** (a) reaction scheme; (b) logarithmically binned 1D histograms of conductance traces for DMEDA and ex-situ synthesized products; (c) representative LC-MS trace of the STM-BJ reaction mixture (* DMEDA and products were derivatized by propionic anhydride for visualization of DMEDA by LC-MS).

We next investigated the source of the *n*-alkyl chain. DMEDA contains a privileged scaffold that enables the cleavage of the central C–C bond, under harsh pyrolysis conditions[14] or oxidative conditions with chemical,[15] photoredox,[16] or electrochemical oxidation.[17] However, measurements of DMEDA isotopologues bearing unnatural isotopes at all possible positions ultimately yielded no detectable isotope incorporation on the alkyl chain in the product (Figure 2a), precluding the fragmentation and reassembly of DMEDA as the source of the *n*-alkyl acylium equivalent.

Based on the observation that we predominately observe *n*-heptanoate (+7 C) of DMEDA when the reaction is run in phenyloctane (octylbenzene, OB) (Figure 3a, SI Figure 4-29, 4-30), we rationalized that this selectivity could originate from the functionalization of the weakest benzylic C–H bond, followed by a formal β-scission event to generate a heptyl fragment which is then trapped by DMEDA (SI Figure 4-36). We subsequently evaluated the hypothesis that functionalization of the solvent was generating the *n*-alkyl acylium. However, we were able to definitively exclude this possibility when we measured deuterium-labeled TD and OB (**3a-c**), and did not detect deuterium incorporation on the product alkyl chain (Figure 2b). Similarly, we determined the presence of an internal standard, 1-methyl-2-phenylindole, did not affect the product distribution, and was unlikely to be the source of the alkyl chain (SI Figure 4-27). Lastly, as all reactions were conducted in air, we evaluated the possible impact of various components of air on the reaction; however, reaction mixtures purged with O_2, CO_2, air, or Ar yielded identical mixtures of products (SI Figure 4-26).

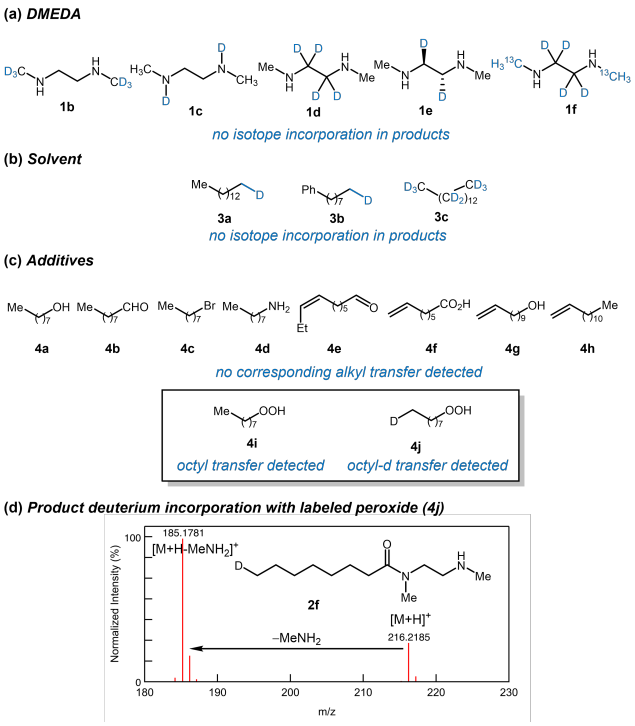

Figure 2. Investigation of the alkyl source. (a) attempted labeling of reaction products with DMEDA isotopologues; (b) attempted labeling of reaction products with solvent isotopologues; (c) attempted labeling of reaction products with additives; (d) mass spectrum of +8 C product showing deuterium incorporation when deuterated hydroperoxide **4j** is added.

The exclusion of all reaction components as the alkyl source necessitated that a trace impurity in the reaction mixture was the alkyl source. We evaluated possible *n*-alkyl precursors bearing functional groups that could conceivably generate an acylium equivalent under reaction conditions. However, alcohol, aldehyde, carboxylic acid, bromide, amine, and alkene were found to be incompetent reagents to transfer alkyl chains (Figure 2c). The empirical observation that fresh TD was orders of magnitude less reactive than older TD that has been exposed to air for longer led us to interrogate autoxidation products as the possible alkyl source (SI Figure 4-29, 4-30). The predominant *n*-heptyl transfer from OB would also be

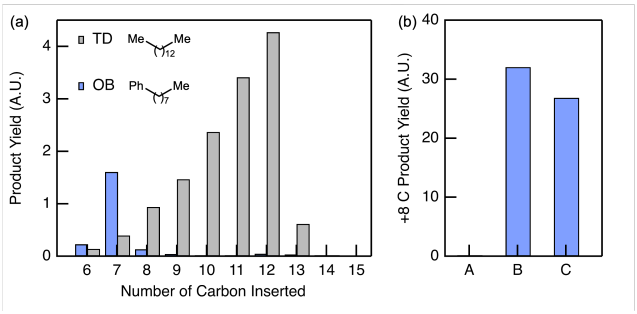

Figure 3. Solvent dependence and surface functionalization. (a) reaction yields in TD and OB; (b) reaction yields when DMEDA is deposited on a gold substrate (A), gold substrate functionalized with DMEDA and *n*-OctOOH **(4i)** then washed (B), and gold substrate functionalized with *n*-OctOOH **(4i)** then washed (C).

consistent with this hypothesis, as the formal benzylic oxidation and β-scission to yield the heptyl fragment would be accelerated by autoxidation.[18] Higher alkanes, such as TD, autoxidize more readily due to the higher presence of secondary C–H bonds;[19] accordingly we then examined hydroperoxides, the primary autoxidation product of *n*-alkanes as the possible alkyl chain precursor.[20–22] While none of the secondary decomposition products of autoxidation, namely alcohol, aldehyde, and carboxylic acids influenced reaction outcome when added exogenously, we discovered that *n*-alkyl hydroperoxides significantly increased the reactivity. Subsequent measurements of a deuterium-labeled hydroperoxide furnished product with the expected isotopic labeling on the product alkyl chain (Figure 2d); this definitively supported the contention that *n*-alkyl hydroperoxides are competent precursors for the alkyl acylium equivalents under reaction conditions.

We observed the same electric field effect with hydroperoxide as an additive in the reaction mixture: reactions in the STM-BJ with mild biases gave increased yields in comparison to ones on gold only (Figure 4). To isolate the effect of the electric field on this reaction from the effect of the gold substrate, the same DMEDA solution was deposited on two steel substrates: one with electric fields applied through the STM-BJ and one without the electric field. Measurements were recorded at the same intervals for comparison. Subsequent analysis of the reaction mixture by LC-MS in Figure 4 showed the reaction in the STM-BJ with applied biases gave increased yield in comparison with steel substrate only.

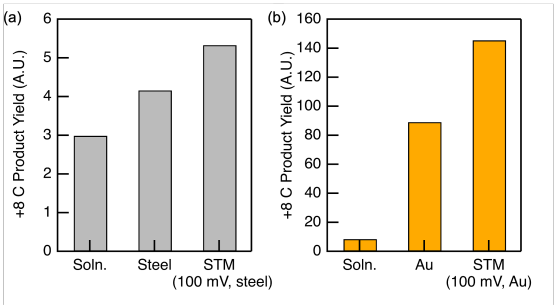

Figure 4. Field dependence. (a) Reaction yields with added *n*-OctOOH in solution only, on steel substrate, and with field at 100 mV in the STM-BJ; (b) reaction yields with added *n*-OctOOH in solution only, on gold substrate, and with field at 100 mV in the STM-BJ.

Intrigued by the apparent high reactivity on the gold surface, we investigated this novel interaction of gold with the hydroperoxide further. We found that functionalization of the gold substrate by the hydroperoxide for a brief contact of 10 s was sufficient, whereupon even after extensive washing of the surface, subsequent addition of DMEDA to the washed substrate could afford detectable products (Figure 3b, SI Figure 4-34). The interaction between the Au substrate and the hydroperoxides could provide a potential pathway for mixtures of hydroperoxides to funnel to their normal alkyl equivalents; we only detect *n*-alkyl amides in this system while autoxidation of hydrocarbons typically generates secondary alkyl hydroperoxides.[19] Gold may also play a role in the C−C cleavage of TD-derived hydroperoxides to generate the shorter normal alkyl chains we observe. (SI Figure 4-36)

In summary, we report that the activation of alkyl hydroperoxide for amine acylation is accelerated by the presence of an EEF. The hydroperoxides, readily generated by autoxidation of higher normal alkanes, were found to efficiently functionalize gold surfaces, and sequester amine coupling partners to afford alkyl amides. This novel field-catalyzed reactivity supports the hypothesis that electric fields accelerate organic reactions by stabilization of charge-separated transition states, and may have implications for the sequestration of hydrocarbon lubricant degradation products to afford value-added normal alkyl amides.

ASSOCIATED CONTENT

Supporting Information.
The supporting information is available free of charge via the Internet at http://pubs.acs.org.

AUTHOR INFORMATION

Corresponding Author

Latha Venkataraman − Department of Chemistry and Department of Applied Physics, Columbia University, New York, New York 10027, United States; orcid.org/00000002-6957-6089; Email: lv2117@columbia.edu
Tomislav Rovis − Department of Chemistry, Columbia University, New York, New York 10027, United States; orcid.org/0000-0001-6287-8669; Email: Tr2504@columbia.edu

Author Contributions

‡ X. W. and B. Z. contributed equally.

Notes

The authors declare no competing financial interest.

ACKNOWLEDGMENT

This work was supported primarily by the NSF CHE-2023568 CCI Phase I: Center for Chemistry with Electric Fields. Research reported in this publication was supported by the Office of The Director, National Institutes of Health of the National Institutes of Health under Award Number S10OD026749. The content is solely the responsibility of the authors and does not necessarily represent the official views of the National Institutes of Health.

REFERENCES

(1) Warshel, A. Electrostatic Basis of Structure-Function Correlation in Proteins. *Acc. Chem. Res.* **1981**, *14* (9), 284–290. https://doi.org/10.1021/ar00069a004.
(2) Warshel, A.; Sharma, P. K.; Kato, M.; Xiang, Y.; Liu, H.; Olsson, M. H. M. Electrostatic Basis for Enzyme Catalysis. *Chem. Rev.* **2006**, *106* (8), 3210–3235. https://doi.org/10.1021/cr0503106.
(3) Shaik, S.; Ramanan, R.; Danovich, D.; Mandal, D. Structure and Reactivity/Selectivity Control by Oriented-External Electric Fields. *Chem. Soc. Rev.* **2018**, *47* (14), 5125–5145. https://doi.org/10.1039/C8CS00354H.
(4) Shaik, S.; Danovich, D.; Joy, J.; Wang, Z.; Stuyver, T. Electric-Field Mediated Chemistry: Uncovering and Exploiting the Potential of (Oriented) Electric Fields to Exert Chemical Catalysis and Reaction Control. *J. Am. Chem. Soc.* **2020**, *142* (29), 12551–12562. https://doi.org/10.1021/jacs.0c05128.

(5) Fried, S. D.; Boxer, S. G. Measuring Electric Fields and Noncovalent Interactions Using the Vibrational Stark Effect. *Acc. Chem. Res.* **2015**, *48* (4), 998–1006. https://doi.org/10.1021/ar500464j.

(6) Fried, S. D.; Boxer, S. G. Electric Fields and Enzyme Catalysis. *Annual Review of Biochemistry* **2017**, *86* (1), 387–415. https://doi.org/10.1146/annurev-biochem-061516-044432.

(7) Ciampi, S.; Darwish, N.; Aitken, H. M.; Díez-Pérez, I.; Coote, M. L. Harnessing Electrostatic Catalysis in Single Molecule, Electrochemical and Chemical Systems: A Rapidly Growing Experimental Tool Box. *Chem. Soc. Rev.* **2018**, *47* (14), 5146–5164. https://doi.org/10.1039/C8CS00352A.

(8) Léonard, N. G.; Dhaoui, R.; Chantarojsiri, T.; Yang, J. Y. Electric Fields in Catalysis: From Enzymes to Molecular Catalysts. *ACS Catal.* **2021**, *11* (17), 10923–10932. https://doi.org/10.1021/acscatal.1c02084.

(9) Ramanan, R.; Danovich, D.; Mandal, D.; Shaik, S. Catalysis of Methyl Transfer Reactions by Oriented External Electric Fields: Are Gold–Thiolate Linkers Innocent? *J. Am. Chem. Soc.* **2018**, *140* (12), 4354–4362. https://doi.org/10.1021/jacs.8b00192.

(10) Shaik, S.; de Visser, S. P.; Kumar, D. External Electric Field Will Control the Selectivity of Enzymatic-Like Bond Activations. *J. Am. Chem. Soc.* **2004**, *126* (37), 11746–11749. https://doi.org/10.1021/ja047432k.

(11) Meir, R.; Chen, H.; Lai, W.; Shaik, S. Oriented Electric Fields Accelerate Diels–Alder Reactions and Control the Endo/Exo Selectivity. *ChemPhysChem* **2010**, *11* (1), 301–310. https://doi.org/10.1002/cphc.200900848.

(12) Aragonès, A. C.; Haworth, N. L.; Darwish, N.; Ciampi, S.; Bloomfield, N. J.; Wallace, G. G.; Diez-Perez, I.; Coote, M. L. Electrostatic Catalysis of a Diels–Alder Reaction. *Nature* **2016**, *531* (7592), 88–91. https://doi.org/10.1038/nature16989.

(13) Zang, Y.; Zou, Q.; Fu, T.; Ng, F.; Fowler, B.; Yang, J.; Li, H.; Steigerwald, M. L.; Nuckolls, C.; Venkataraman, L. Directing Isomerization Reactions of Cumulenes with Electric Fields. *Nat. Commun.* **2019**, *10* (1), 4482. https://doi.org/10.1038/s41467-019-12487-w.

(14) Werstiuk, N. H. Thermolysis of N-Alkylated Ethylenediamines: An Ultraviolet Photoelectron Spectroscopy Study. *Can. J. Chem.* **1986**, *64* (11), 2175–2183. https://doi.org/10.1139/v86-358.

(15) Sun, W.; Lin, H.; Zhou, W.; Li, Z. Oxidative Ortho-Amino-Methylation of Phenols via C–H and C–C Bond Cleavage. *RSC Adv.* **2014**, *4* (15), 7491–7494. https://doi.org/10.1039/C3RA46373G.

(16) Sartoria, P.; Velayutham, D.; Ignat'eva, N.; Noel, M. Electrochemical Fluorination of N,N,N′,N′-Tetramethylethylenediamine. *Journal of Fluorine Chemistry* **1997**, *83* (1), 1–8. https://doi.org/10.1016/S0022-1139(97)00002-X.

(17) Cai, S.; Zhao, X.; Wang, X.; Liu, Q.; Li, Z.; Wang, D. Z. Visible-Light-Promoted C-C Bond Cleavage: Photocatalytic Generation of Iminium Ions and Amino Radicals. *Angew. Chem. Int. Ed.* **2012**, *51* (32), 8050–8053. https://doi.org/10.1002/anie.201202880.

(18) Ingold, K. U. Peroxy Radicals. *Acc. Chem. Res.* **1969**, *2* (1), 1–9. https://doi.org/10.1021/ar50013a001.

(19) Sheldon, R. A. Synthesis and Uses of Alkyl Hydroperoxides and Dialkyl Peroxides. In *Peroxides (1983)*; John Wiley & Sons, Ltd, 1983; pp 161–200. https://doi.org/10.1002/9780470771730.ch6.

(20) Blaine, S.; Savage, P. E. Reaction Pathways in Lubricant Degradation. 1. Analytical Characterization of n-Hexadecane Autoxidation Products. *Ind. Eng. Chem. Res.* **1991**, *30* (4), 792–798. https://doi.org/10.1021/ie00052a026.

(21) Blaine, S.; Savage, P. E. Reaction Pathways in Lubricant Degradation. 2. n-Hexadecane Autoxidation. *Ind. Eng. Chem. Res.* **1991**, *30* (9), 2185–2191. https://doi.org/10.1021/ie00057a020.

(22) Blaine, S.; Savage, P. E. Reaction Pathways in Lubricant Degradation. 3. Reaction Model for n-Hexadecane Autoxidation. *Ind. Eng. Chem. Res.* **1992**, *31* (1), 69–75. https://doi.org/10.1021/ie00001a010.

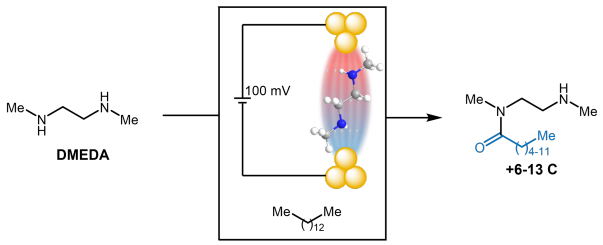
Me
N
H
H
N
Me
DMEDA
100 mV
Me
12
Me
Me
N
H
N
Me
O
Me
4-11
+6-13 C